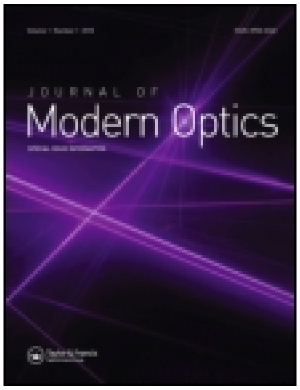

Journal of Modern Optics
Publication details, including instructions for authors and subscription information:
http://www.tandfonline.com/loi/tmop20

Aluminum diffuser of Lambert scattering and high reflectivity based on abrasion and sodium hydroxide corrosion

Bo Li [a b] , Shurong Wang [a] & Yu Huang [b]

[a] Changchun Institute of Optics, Fine Mechanics and Physics, Chinese Academy of Sciences, Changchun, Jilin 130033, China

[b] Graduate School of the Chinese Academy of Sciences, Beijing 100039, China

Version of record first published: 10 Aug 2010.

To cite this article: Bo Li, Shurong Wang & Yu Huang (2010): Aluminum diffuser of Lambert scattering and high reflectivity based on abrasion and sodium hydroxide corrosion, Journal of Modern Optics, 57:13, 1189-1193

To link to this article: http://dx.doi.org/10.1080/09500340.2010.506249

Journal of Modern Optics
Vol. 57, No. 13, 20 July 2010, 1189–1193

Aluminum diffuser of Lambert scattering and high reflectivity based on abrasion and sodium hydroxide corrosion

Bo Li[a,b], Shurong Wang[a]* and Yu Huang[b]

[a]*Changchun Institute of Optics, Fine Mechanics and Physics, Chinese Academy of Sciences, Changchun, Jilin 130033, China;* [b]*Graduate School of the Chinese Academy of Sciences, Beijing 100039, China*

(*Received 8 April 2010; final version received 22 June 2010*)

We discover that an aluminum surface roughened with 30–70 μm carborundum abrasive gets Lambert scattering properties and a higher hemisphere reflectivity after being corroded with sodium hydroxide solution. Experimental results demonstrate that the scattering properties of the corroded aluminum surface conform to the Lambert cosine law at normal incidence and the hemisphere reflectivity is obviously improved in the 250–1500 nm spectrum range.

Keywords: diffuser; hemisphere reflectivity; measurement

1. Introduction

Solar diffusers are frequently used for the onboard calibration of reflective solar bands in space-born remote sensing radiometers [1–4]. The onboard calibration of radiometric measurements in remote sensing is achieved by observation of a sun-illuminated reflectance secondary standard using previously calibrated reflecting diffusers [5–7]. The aluminum diffuser is widely used in the field of space optical instrument and radiometric calibration because of its high reflectivity and perfect stability in the space environment. Currently, there are two typical fabrication methods to process aluminum diffusers – abrasion and sandblasting; however, compared with the diffusers made with BaSO4 and Teflon, which have a approximate Lambert surface, aluminum diffusers have bad scattering properties and satisfactory stability of reflectance [8–10]. This will increase the probable error of the optical instrument and radiometric calibration [11–15]; therefore, the aluminum surface with Lambert scattering is very significant in the improvement of relevant instrument performance.

In this paper, we propose a method based on abrasion and chemical corrosion to acquire Lambert scattering on an aluminum surface. We found that the roughened aluminum surface conformed to the Lambert cosine law, and then we measured the hemisphere reflectivities of aluminum with Lambda 950, and found that the hemisphere reflectivity was improved in the 50–1500 nm spectrum range. The proposed fabrication method of the aluminum diffuser includes two procedures, abrasion and chemical corrosion.

2. Methodology

Abrasion is the primary procedure in the method we used. The base plates are machined from aluminum 5083, which is known for exceptional performance in extreme environments and is highly resistant to the attack of seawater and industrial chemical environments. The plates were roughened with 30–70 μm aluminum oxide abrasive to yield a visually uniform surface. The samples were then cleaned according to the following procedure: first they were immersed in trichloroethane in an ultrasonic cleaner, followed by similar immersion in Freon TF. They were then soaked in a water and alcohol bath, then rinsed thoroughly with hot distilled water and, finally, rinsed once more with triple-distilled acetone to remove all water. This procedure removes some but not all contaminants deposited on the aluminum surface because the aluminum particles produced by abrasion and the microsize abrasive were hardly clean, but it could not make the surface form an approximate Lambert surface.

Next, we deal with the round surface through chemical corrosion. The diffuser was immersed in NaOH solution. It was a galvano-chemistry procedure, the roughened aluminum sample was eroded equably in lye, and the result is $NaAlO_2$. Chemical corrosion could sweep the gray abrasion residue, which was composed of aluminum powder and abrasives.

*Corresponding author. Email: libo0008429@163.com

ISSN 0950–0340 print/ISSN 1362–3044 online

DOI: 10.1080/09500340.2010.506249
http://www.informaworld.com

In addition, the diffusion velocity of lye is faster at the microscopic peak of the aluminum surface than that at the valley because of the lye's viscosity in this process. So the chemical corrosion has the function of leveling the surface. After chemical corrosion, there were black contaminations on the corroded aluminum surface, so we repeated the bath procedure of abrasion again, until finally the diffusers had a homogeneous, smoothing and scattering surface.

The temperatures, reaction time and concentration of NaOH are key factors for the chemical corrosion. We discovered through experiments that the aluminum surface has Lambert scattering properties when NaOH concentration is 55 g/l, initial temperature 60°C, and reaction time 150 s.

3. Measurement

3.1. Scattering properties

We measured the scattering property of the two kinds of diffusers (abrased and corroded) with a monochromator and a goniometer: the sizes of the two diffusers are 90 mm × 60 mm. Figure 1(*a*) shows a schematic view of the measurement setup for the radiation patterns of the aluminum diffusers. The homogeneous light of the monochromator was collimated by two spherical mirrors and was then used as the incidence beam of the sample. The goniometer has two rotation gears to adjust the sample incidence and detector acceptance angle from 0° to 270°, respectively. The photodetector was placed 300 mm from the sample.

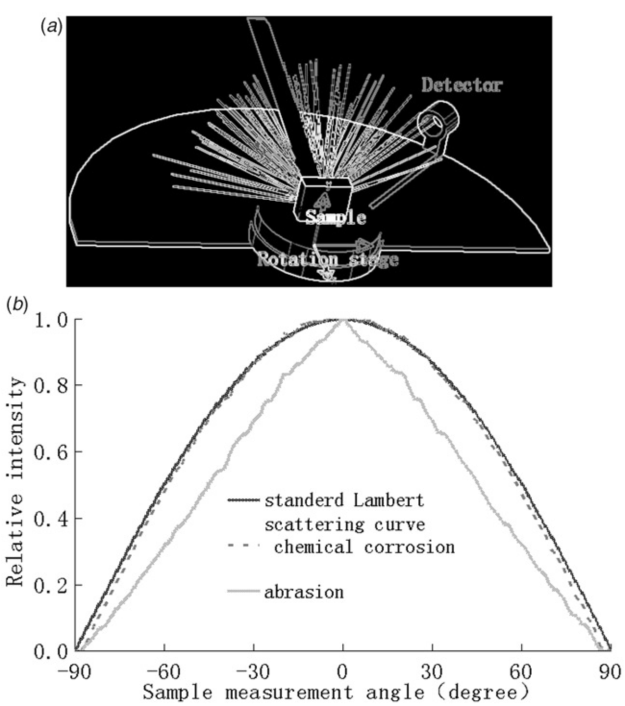

Figure 1. (*a*) The schematic view of the measurement setup for the radiation patterns of the aluminum diffusers. (*b*) The scattering properties of the two kinds of aluminum surfaces at normal incidence.

For the Lambert scattering, the diffuser's radiance is equivalent in any reflective direction, and conforms to the Lambert cosine law. The relations between detector signal and irradiance satisfy Equation (1)

$$R_E = I/E\left[\mathrm{A/W\,m^2}\right] \quad (1)$$

R_E is the current's response to irradiance, I is the current of detector, and E is the irradiance of the deflector. According to the principle of Lambert scattering, E satisfies Equation (2).

$$E(\theta) = E_{\mathrm{nor}}\cos(\theta) \quad (2)$$

where $E(\theta)$ is the sample irradiance in the θ direction, and E_{nor} is the sample irradiance in the normal direction. We can acquire the following relations from Equations (1) and (2):

$$I(\theta) = I_{\mathrm{nor}}\cos(\theta) \quad (3)$$

where $I(\theta)$ is the detector signal in the θ direction, and I_{nor} is the detector signal in the normal direction.

The Lambert scattering sample satisfies Equation (3). Figure 1(*b*) shows the measurement result of the two samples at 300 nm wavelength and, to easily distinguish the Lambert cosine scattering properties, the signal value of the detector has been normalized with the cosine. We can see that the abrased aluminum diffuser has strong Lambert scattering properties after being corroded by lye, and which conform to the Lambert cosine law at normal incidence.

3.2. Hemisphere reflectivity

We measured the hemisphere reflectivities of the two surfaces with a LAMBDA 950 UV-VIS-NIR spectrophotometer. The LAMBDA 950 is one of highest performance UV/VIS/NIR systems. There are two accessories for the Lambda 950: the Universal Reflectance Accessory (URA) and a 150 mm integrating sphere. The 150 mm integrating sphere is an internal diffuse reflectance accessory, which can be used to collect the total and diffuse reflectance of both specular and diffuse samples, utilizing wavelengths between 2500 nm–200 nm. We measured the hemisphere reflectivity in the 250 nm–1500 nm spectral range, 0.5 nm bandpass and 5 nm interval wave.

The measurement results show that the hemisphere reflectivity of the chemical corrosion diffuser is obviously high in the 250 nm–1500 nm wavelength range compared with the abrasion diffuser. Figure 2 shows the measurement results of the LAMBDA 950.

3.3. *Microstructure and composition*

To get more information about the relation between the formations of the corrosion diffuser and the optical performances, we observed images of the two diffusers with a scanning electron microscopy (SEM) at different magnifications. Figure 3(*a*) and (*b*) show the diffuser surfaces based on abrasion and chemical corrosion, respectively, in 3.5 k × magnification. We can easily find that the aluminum surface based on chemical corrosion was smoother and cleaner than that based on abrasion, on which there is much fragmental deposit on the surface. Figure 3(*c*) and (*d*) show the diffuser surfaces based on abrasion and chemical corrosion, respectively, in 200 k × magnification. There are many black apertures on the aluminum surface based on abrasion, but the apertures disappear after chemical corrosion. The roughness of the three kinds of diffuser's surface is contrasted in Figure 4. A KLA Tencor P-16+ surface profiler is used to measure the roughness of the diffuser's surface. The results show that the surface roughness of corrosion aluminum reduces significantly, and the RMS of abrasion, corrosion and $BaSO_4$ is 5.74 μm, 2.07 μm and 1.58 μm, respectively. We analyzed that the fragmental deposit and black apertures shape the micro light trap that reduces the reflectivity and Lambert scattering, and that the corrosion made the micro peaks and valleys of the aluminum surface random, so the scattering properties and the reflectivity were improved after corrosion.

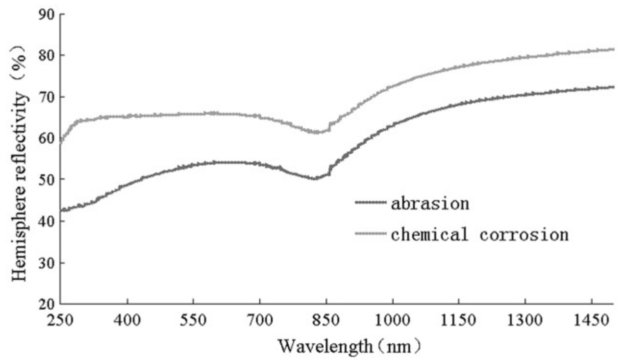

Figure 2. The hemisphere reflectivities of the abrasion and chemical corrosion aluminum surfaces.

We identified the chemical composition of abrasion and chemical-corrosion roughened surfaces with energy dispersive spectroscopy (EDS). Aluminum 5083 chemical composition for aluminum alloy 5083 is made typically of three elements: Al, Si, and Mg, and

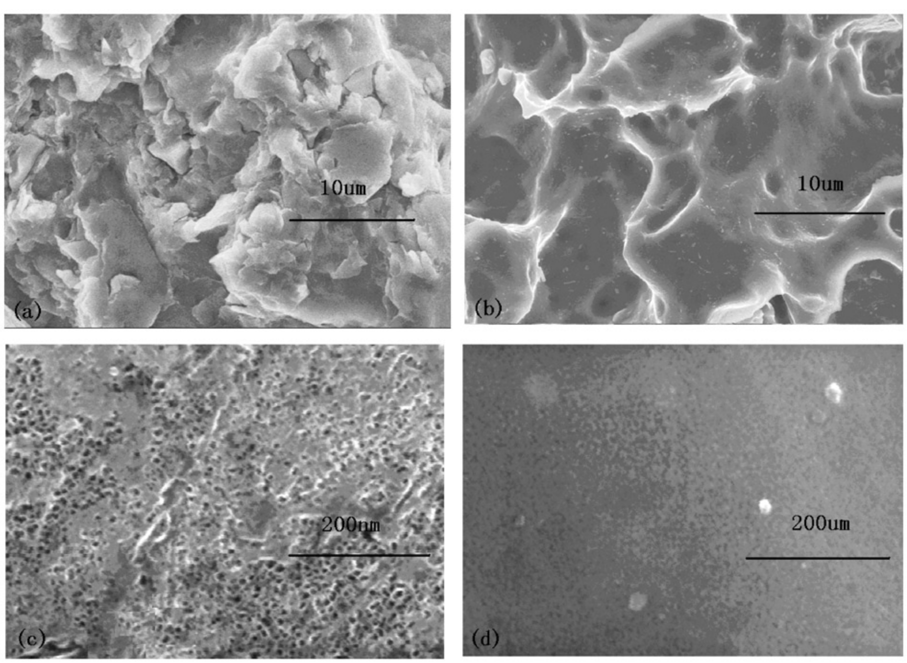

Figure 3. SEM images of the diffuser. (*a*) The surface image in 3.5 k × magnification with abrasion. (*b*) The surface image in 3.5 k × magnification with chemical corrosion. (*c*) The surface image in 200 k × magnification with abrasion. (*d*) The surface image in 200 k × magnification with chemical corrosion.

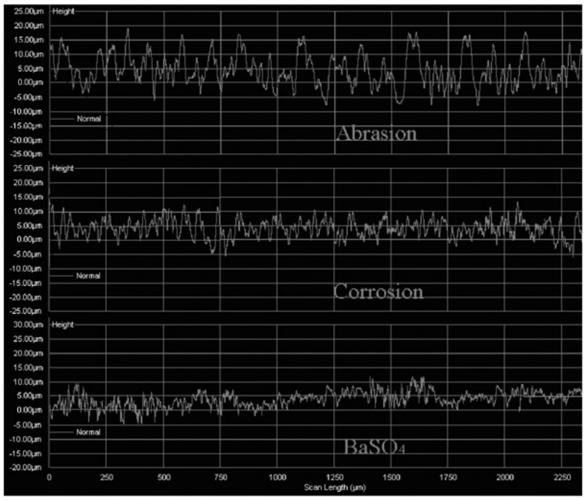

Figure 4. The surface roughness of three kinds of diffusers.

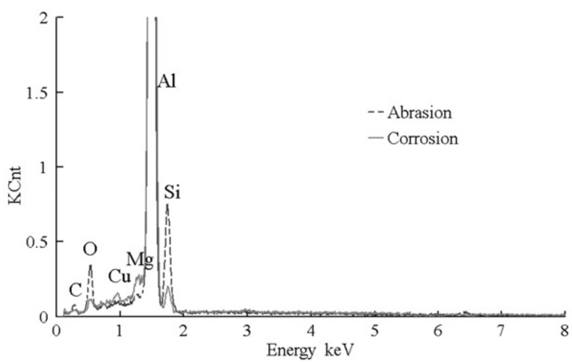

Figure 5. The chemical composition of the abrasion and chemical-corrosion roughened surfaces with EDS.

Table 1. The chemical composition of the abrasion and chemical corrosion diffuser.

Element	Wt(b)%	Wt(a)%
C	0.03	0.01
O	7.60	1.40
Cu	0.43	0.89
Mg	0.50	1.13
Al	78.69	94.39
Si	12.65	2.18

the carborundum is made of SiC, SiO_2, and Al_2O_3. Figure 5 shows the chemical composition of the abrasion and corrosion aluminum surfaces. We can see that the content of C, Si, Fe and O reduce significantly for the corroded aluminum surface; the results analyzed by EDS show that the weight of aluminum on the rough surface has changed from 78.69% of abrasion to 94.39% of corrosion (Table 1), the Si has changed from 12.65% to 2.18%, and the O has changed from 7.6% to 1.4%. For the 1.4% weight of O, we analyzed that the aluminum was oxidized partly when the diffuser of corrosion was in the air. These figures demonstrate that the abrasion residue (SiC, SiO_2 and Al_2O_3) has been cleaned out mostly by corrosion.

4. Conclusion

In this paper, we proposed a corrosion method for an aluminum diffuser, a method based on traditional abrasion. We analyzed the principle of lye corrosion at first, and then we studied the corrosion diffuser and abrasion diffuser with a series of experiments (cosine radiation property measurement, hemisphere measurement, microstructure observing and chemical composition analysis). The experiment results show that the NaOH corrosion changes the microstructure of the abrasion aluminum surface and the ultrasonic vibrations can clean out the various residues after corrosion, although that is impossible for an abrasion aluminum diffuser. The microstructure change of corrosion makes the diffuser have Lambert scattering (normal incidence), and the reduction of residues improves 13% on the average hemisphere reflectivity, from 250 nm–1500 nm for the abrasion diffuser. This will improve the calibration precision of the optical sensing instrument.

Acknowledgements

The authors acknowledge financial support from the National Natural Science Foundation of China (Grant No. 40675083), and Professor Futian Li for fruitful discussion and critical feedback.

References

[1] Xiong, X.; Erives, H.; Xiong, S.; Xie, X.; Esposito, J.; Sun, J.; Barnes, W. *SPIE Proc*. **2005,** *5882,* 261.
[2] Gröbner, J.; Blumthaler, M. *Opt. Lett* **2007,** *32,* 80–82.
[3] Li, Z.; Zhao, X.; Kahn, R.; Mishchenko, M.; Remer, L.; Lee, K.H.; Wang, M.; Laszlo, I.; Nakajima, T.; Maring, H. *Ann. Geophys*. **2009,** *27,* 2755–2770.
[4] Eplee, R.E. Jr; Patt, F.S.; Barnes, R.A.; McClain, C.R. *Appl. Opt*. **2007,** *46,* 762–773.
[5] Jäkel, E.; den Outer, P.N.; Tax, R.B.; Görts, PC.; Reinen, H.A.J.M. *Appl. Opt*. **2007,** *46,* 4222–4227.
[6] Georgiev, G.T.; Butler, J.J. *Appl. Opt*. **2007,** *46,* 7892–7899.
[7] van Brug, H.; Bazalgette Courrèges-Lacoste, G.; Groote Schaarsberg, J.; Otter, G.; Del Bello, U.; Snijders, B. *SPIE Proc*. **2005,** *5882,* 202.

[8] Yasuji, Y.; Takahiro, K.; Shigetaka, M. *Proceedings of the Japanese Conference on Remote Sensing*, **2002,** *33*, 87–90.
[9] Fleming, J.C. *SPIE Proc*. **2006,** *2864,* 406–415.
[10] Fowler, W.K.; Nelson, V.W. *Metrologia* **1993,** *30,* 255.
[11] Xiong, X.; Murphy, R.; Sun, J.; Esposito, J.; Barnes, W.; Guenther, B. *IEEE Proc. IGARSS'03*. **2003,** *5,* 3043–3045.
[12] Lee III, R.B.; Avis, L.M.; Gibson, M.A.; Kopia, L.P. *Appl. Opt*. **1992,** *46,* 6643–6652.
[13] Naulleau, P.P.; Liddle, J.A.; Salmassi, F.; Anderson, E.H.; Gullikson, E.M. *Appl. Opt*. **2004,** *43,* 5323–5329.
[14] Massera, E.; Rea, I.; Nasti, I.; Maddalena, P.; Di Francia, G. *Appl. Opt*. **2006,** *45,* 6746–6749.
[15] Bazalgette Courrèges-Lacoste G., van Brug, H., Otter, G. In Proceedings of the 2nd Working Meeting on MERIS and AATSR Calibration and Geophysical Validation (MAVT-2006), Frascati, Italy, Jul, 2006; Danesy, D., Ed.; ESA Publications: Noordwijk, 2006.